

1 **MitoChime: A Machine-Learning Pipeline for**
2 **Detecting PCR-Induced Chimeras in**
3 **Mitochondrial Illumina Reads**

4 A Special Project Proposal
5 Presented to
6 the Faculty of the Division of Physical Sciences and Mathematics
7 College of Arts and Sciences
8 University of the Philippines Visayas
9 Miag-ao, Iloilo

10 In Partial Fulfillment
11 of the Requirements for the Degree of
12 Bachelor of Science in Computer Science

13 by

14 Duranne Duran
15 Yvonne Lin
16 Daniella Pailden

17 Adviser
18 Francis Dimzon

19 November 25, 2025

Contents

21	1 Introduction	1
22	1.1 Overview	1
23	1.2 Problem Statement	3
24	1.3 Research Objectives	4
25	1.3.1 General Objective	4
26	1.3.2 Specific Objectives	4
27	1.4 Scope and Limitations of the Research	5
28	1.5 Significance of the Research	6
29	2 Review of Related Literature	7
30	2.1 The Mitochondrial Genome	7
31	2.1.1 Mitochondrial Genome Assembly	8

32	2.2 PCR Amplification and Chimera Formation	9
33	2.2.1 Effects of Chimeric Reads on Organelle Genome Assembly	10
34	2.3 Existing Traditional Approaches for Chimera Detection	11
35	2.3.1 UCHIME	12
36	2.3.2 UCHIME2	14
37	2.3.3 CATch	16
38	2.3.4 ChimPipe	17
39	2.4 Machine Learning Approaches for Chimera and Sequence Quality	
40	Detection	18
41	2.4.1 Feature-Based Representations of Genomic Sequences . . .	18
42	2.5 Synthesis of Chimera Detection Approaches	20
43	3 Research Methodology	25
44	3.1 Research Activities	25
45	3.1.1 Data Collection	26
46	3.1.2 Data Simulation	27
47	3.1.3 Bioinformatics Tools Pipeline	28
48	3.1.4 Machine-Learning Model Development	31

49	3.1.5 Validation and Testing	32
50	3.1.6 Documentation	32
51	3.2 Calendar of Activities	33

⁵² List of Figures

⁵³	3.1 Process Diagram of Special Project	26
---------------	--	----

54 List of Tables

⁵⁷ **Chapter 1**

⁵⁸ **Introduction**

⁵⁹ **1.1 Overview**

⁶⁰ The rapid advancement of next-generation sequencing (NGS) technologies has
⁶¹ transformed genomic research by enabling high-throughput and cost-effective
⁶² DNA analysis (Metzker, 2010). Among current platforms, Illumina sequencing
⁶³ remains the most widely adopted, capable of producing millions of short reads
⁶⁴ that can be assembled into reference genomes or analyzed for genetic variation
⁶⁵ (Bentley et al., 2008; Glenn, 2011). Despite its high base-calling accuracy,
⁶⁶ Illumina sequencing is prone to artifacts introduced during library preparation,
⁶⁷ particularly polymerase chain reaction (PCR)-induced chimeras, which are ar-
⁶⁸ tificial hybrid sequences that do not exist in the true genome (Judo, Wedel, &
⁶⁹ Wilson, 1998).

⁷⁰ PCR chimeras form when incomplete extension products from one template

71 anneal to an unrelated DNA fragment and are extended, creating recombinant
72 reads (Qiu et al., 2001). In mitochondrial genome assembly, such artifacts are
73 especially problematic because the mitochondrial genome is small, circular, and
74 often repetitive (Boore, 1999; Cameron, 2014). Even a small number of chimeric
75 or mis-joined reads can reduce assembly contiguity and introduce false junctions
76 during organelle genome reconstruction (Dierckxsens, Mardulyn, & Smits, 2017;
77 Hahn, Bachmann, & Chevreux, 2013; Jin et al., 2020). Existing assembly tools
78 such as GetOrganelle and MITObim assume that input reads are largely free of
79 such artifacts (Hahn et al., 2013; Jin et al., 2020). Consequently, undetected
80 chimeras may produce fragmented assemblies or misidentified organellar bound-
81 aries. To ensure accurate reconstruction of mitochondrial genomes, a reliable
82 and automated method for detecting and filtering PCR-induced chimeras before
83 assembly is essential.

84 This study focuses on mitochondrial sequencing data from the genus *Sar-*
85 *dinella*, a group of small pelagic fishes widely distributed in Philippine waters.
86 Among them, *Sardinella lemuru* (Bali sardinella) is one of the country's most
87 abundant and economically important species, providing protein and livelihood
88 to coastal communities (Labrador, Agmata, Palermo, Ravago-Gotanco, & Pante,
89 2021; Willette, Bognot, Mutia, & Santos, 2011). Accurate mitochondrial assem-
90 blies are critical for understanding its population genetics, stock structure, and
91 evolutionary history. However, assembly pipelines often encounter errors or fail
92 to complete due to undetected chimeric reads. To address this gap, this research
93 introduces **MitoChime**, a machine-learning pipeline designed to detect and filter
94 PCR-induced chimeric reads using both alignment- and sequence-derived statisti-
95 cal features. The tool aims to provide bioinformatics laboratories, particularly the

₉₆ Philippine Genome Center Visayas, with an efficient, interpretable, and resource-
₉₇ optimized solution for improving mitochondrial genome reconstruction.

₉₈ 1.2 Problem Statement

₉₉ While NGS technologies have revolutionized genomic data acquisition, the ac-
₁₀₀ curacy of mitochondrial genome assembly remains limited by artifacts produced
₁₀₁ during PCR amplification. These chimeric reads can distort assembly graphs and
₁₀₂ cause misassemblies, with especially severe effects in small, circular mitochon-
₁₀₃ drial genomes (Boore, 1999; Cameron, 2014). Existing assembly pipelines such
₁₀₄ as GetOrganelle, MITObim, and NOVOPlasty assume that sequencing reads are
₁₀₅ free of such artifacts (Dierckxsens et al., 2017; Hahn et al., 2013; Jin et al., 2020).
₁₀₆ At the Philippine Genome Center Visayas, several mitochondrial assemblies have
₁₀₇ failed or yielded incomplete contigs despite sufficient coverage, suggesting that
₁₀₈ undetected chimeric reads compromise assembly reliability. Meanwhile, exist-
₁₀₉ ing chimera-detection tools such as UCHIME and VSEARCH were developed
₁₁₀ primarily for amplicon-based microbial community analysis and rely heavily on
₁₁₁ reference or taxonomic comparisons (Edgar, Haas, Clemente, Quince, & Knight,
₁₁₂ 2011; Rognes, Flouri, Nichols, Quince, & Mahé, 2016). These approaches are un-
₁₁₃ suitable for single-species organellar data, where complete reference genomes are
₁₁₄ often unavailable. Therefore, there is a pressing need for a reference-independent,
₁₁₅ data-driven tool capable of automatically detecting and filtering PCR-induced
₁₁₆ chimeras in mitochondrial sequencing datasets.

₁₁₇ **1.3 Research Objectives**

₁₁₈ **1.3.1 General Objective**

₁₁₉ To develop and evaluate a machine-learning-based pipeline (MitoChime) capa-
₁₂₀ ble of detecting PCR-induced chimeric reads in *Sardinella lemuru* mitochondrial
₁₂₁ sequencing data to improve the accuracy of mitochondrial genome assembly.

₁₂₂ **1.3.2 Specific Objectives**

₁₂₃ Specifically, the researchers aim to:

- ₁₂₄ 1. Construct empirical as well as simulated *Sardinella lemuru* Illumina paired-end datasets containing both clean and PCR-induced chimeric reads.
- ₁₂₆ 2. Extract alignment and sequence-based features such as k-mer composition, junction complexity, split-alignment counts from both clean and chimeric reads.
- ₁₂₉ 3. Train, validate, and compare supervised machine-learning models for classifying reads as clean or chimeric.
- ₁₃₁ 4. Determine feature importance and identify the most informative indicators of PCR-induced chimerism.
- ₁₃₃ 5. Integrate the optimized classifier into a modular and interpretable pipeline deployable on standard computing environments at PGC Visayas.

135 1.4 Scope and Limitations of the Research

136 This study focuses on detecting PCR-induced chimeric reads in Illumina paired-
137 end mitochondrial sequencing data from the *Sardinella lemuru* species. The deci-
138 sion to limit the taxonomic scope is motivated by three factors: (1) To provide a
139 biologically coherent system by eliminating interspecific variation, such as differ-
140 ences in mitochondrial genome size, GC content, and repetitive regions. Restrict-
141 ing the analysis to *S. lemuru* reduces biological noise and ensures that observed
142 patterns reflect chimeric artifacts rather than taxonomic differences. (2) The se-
143 lected species is directly relevant to ongoing research initiatives and sequencing
144 efforts at the Philippine Genome Center Visayas, making it a strategically ap-
145 propriate choice for developing and validating the analytical framework; and (3)
146 *Sardinella lemuru* possesses a moderately complex but well-characterized mito-
147 chondrial genome, with clear gene boundaries and sufficient publicly available
148 data from repositories such as the National Center for Biotechnology Information
149 (NCBI).

150 The study emphasizes `wgsim`-based simulations and selected empirical mito-
151 chondrial datasets. It excludes naturally occurring chimeras, nuclear mitochon-
152 drial pseudogenes (NUMTs), and large-scale structural rearrangements in nuclear
153 genomes. Feature extraction prioritizes interpretable, shallow statistics and align-
154 ment metrics rather than deep-learning embeddings to ensure transparency and
155 computational efficiency. Testing on long-read platforms (e.g., Nanopore, PacBio)
156 and other taxa lies beyond the project's scope. The resulting pipeline will serve
157 as a foundation for future, broader chimera-detection frameworks applicable to
158 diverse organellar genomes.

¹⁵⁹ 1.5 Significance of the Research

¹⁶⁰ This research provides both methodological and practical contributions to mi-
¹⁶¹tochondrial genomics and bioinformatics. First, MitoChime enhances assembly
¹⁶²accuracy by filtering PCR-induced chimeras prior to genome assembly, thereby
¹⁶³improving the contiguity and correctness of *Sardinella lemuru* mitochondrial
¹⁶⁴genomes. Second, it promotes automation and reproducibility by replacing
¹⁶⁵subjective manual curation with a data-driven, machine-learning-based work-
¹⁶⁶flow. Third, the pipeline demonstrates computational efficiency through its
¹⁶⁷design, enabling implementation on modest computing infrastructures commonly
¹⁶⁸available in regional laboratories. Beyond technical improvements, MitoChime
¹⁶⁹contributes to local capacity building by strengthening expertise in bioinformatics
¹⁷⁰and machine-learning integration, aligning with the mission of the Philippine
¹⁷¹Genome Center Visayas. Finally, accurate mitochondrial assemblies are vital
¹⁷²for fisheries management, population genetics, and biodiversity conservation,
¹⁷³providing reliable genomic resources for species such as *S. lemuru*. Through
¹⁷⁴these contributions, MitoChime advances the reliability of mitochondrial genome
¹⁷⁵reconstruction and supports sustainable, data-driven research in Philippine
¹⁷⁶genomics.

¹⁷⁷ **Chapter 2**

¹⁷⁸ **Review of Related Literature**

¹⁷⁹ This chapter presents an overview of the literature relevant to the study. It
¹⁸⁰ discusses the biological and computational foundations underlying mitochondrial
¹⁸¹ genome analysis and assembly, as well as existing tools, algorithms, and techniques
¹⁸² related to chimera detection and genome quality assessment. The chapter aims to
¹⁸³ highlight the strengths, limitations, and research gaps in current approaches that
¹⁸⁴ motivate the development of the present study.

¹⁸⁵ **2.1 The Mitochondrial Genome**

¹⁸⁶ Mitochondrial genome (mtDNA) is a small, typically circular molecule found in
¹⁸⁷ most eukaryotes. It encodes essential genes involved in oxidative phosphorylation
¹⁸⁸ and energy metabolism. Because of its conserved structure and maternal inher-
¹⁸⁹ itance, mtDNA has become a valuable genetic marker for studies in evolution,
¹⁹⁰ population genetics, and phylogenetics (Anderson et al., 1981; Boore, 1999). In

191 animal species, the mitochondrial genome ranges from 15–20 kilobase and contains
192 13 protein-coding genes, 22 tRNAs, and two rRNAs arranged compactly without
193 introns (Gray, 2012). In comparison to nuclear DNA the ratio of the number
194 of copies of mtDNA is higher and has relatively simple organization which make
195 it particularly suitable for genome sequencing and assembly studies (Dierckxsens
196 et al., 2017). Moreover, mitochondrial genomes provide crucial insights into evo-
197 lutionary relationships among species and are increasingly used for testing new
198 genomic assembly and analysis methods.

199 2.1.1 Mitochondrial Genome Assembly

200 Mitochondrial genome assembly refers to the reconstruction of the complete mito-
201 chondrial DNA (mtDNA) sequence from raw or fragmented sequencing reads. It is
202 conducted to obtain high-quality, continuous representations of the mitochondrial
203 genome that can be used for a wide range of analyses, including species identi-
204 fication, phylogenetic reconstruction, evolutionary studies, and investigations of
205 mitochondrial diseases. Because mtDNA evolves relatively rapidly and is mater-
206 nally inherited, its assembled sequence provides valuable insights into population
207 structure, lineage divergence, and adaptive evolution across taxa (Boore, 1999).
208 Compared to nuclear genome assembly, assembling the mitochondrial genome is
209 often considered more straightforward but still encounters distinct technical chal-
210 lenges such as sequencing errors, low coverage regions, and chimeric reads that can
211 distort the final assembly, leading to incomplete or misassembled genomes. These
212 errors can propagate into downstream analyses, emphasizing the need for robust
213 chimera detection and sequence validation methods in mitochondrial genome re-

214 search.

215 2.2 PCR Amplification and Chimera Formation

216 Polymerase Chain Reaction (PCR) plays an important role in next-generation
217 sequencing (NGS) library preparation, as it amplifies target DNA fragments for
218 downstream analysis. However, the amplification process can also introduce arti-
219 facts that affect data accuracy, one of them being the formation of chimeric se-
220 quences. Chimeras typically arise when incomplete extension occurs during a PCR
221 cycle. This causes the DNA polymerase to switch from one template to another
222 and generate hybrid recombinant molecules (Judo et al., 1998). Artificial chimeras
223 are produced through such amplification errors, whereas biological chimeras oc-
224 cur naturally through genomic rearrangements or transcriptional events. These
225 biological chimeras can have functional roles and may encode tissue-specific novel
226 proteins that link to cellular processes or diseases (Frenkel-Morgenstern et al.,
227 2012).

228 In the context of amplicon-based sequencing, PCR-induced chimeras can sig-
229 nificantly distort analytical outcomes. Their presence artificially inflates estimates
230 of genetic or microbial diversity and may cause misassemblies during genome re-
231 construction. (Qin et al., 2023) has reported that chimeric sequences may account
232 for more than 10% of raw reads in amplicon datasets. This artifact tends to be
233 most prominent among rare operational taxonomic units (OTUs) or singletons,
234 which are sometimes misinterpreted as novel diversity, which further causes the
235 complication of microbial diversity analyses (Gonzalez, Zimmermann, & Saiz-

236 Jimenez, 2004). Moreover, the likelihood of chimera formation has been found to
237 vary with the GC content of target sequences, with lower GC content generally
238 associated with a reduced rate of chimera generation (Qin et al., 2023).

239 **2.2.1 Effects of Chimeric Reads on Organelle Genome As-**
240 **sembly**

241 In mitochondrial DNA (mtDNA) assembly workflows, PCR-induced chimeras pose
242 additional challenges. Assembly tools such as GetOrganelle and MitoBeam, which
243 operate under the assumption of organelle genome circularity, are vulnerable when
244 chimeric reads disrupt this circular structure. Such disruptions can lead to assem-
245 bly errors or misassemblies (Bi et al., 2024). These artificial sequences interfere
246 with the assembly graph, which makes it more difficult to accurately reconstruct
247 mitochondrial genomes. In addition, these artifacts propagate false variants and
248 erroneous annotations in genomic data. Hence, determining and minimizing PCR-
249 induced chimera formation is vital for improving the quality of mitochondrial
250 genome assemblies, and ensuring the reliability of amplicon sequencing data.

251 **2.3 Existing Traditional Approaches for Chimera**

252 **Detection**

253 Several computational tools have been developed to identify chimeric sequences in
254 NGS datasets. These tools generally fall into two categories: reference-based and
255 de novo approaches. Reference-based chimera detection, also known as database-
256 dependent detection, is one of the earliest and most widely used computational
257 strategies for identifying chimeric sequences in amplicon-based microbial commu-
258 nity studies. These methods rely on the comparison of each query sequence against
259 a curated, high-quality database of known, non-chimeric reference sequences to
260 determine whether the query can be more plausibly explained as a composite or
261 a mosaic of two or more reference sequences rather than as a genuine biological
262 variant (Edgar et al., 2011).

263 On the other hand, the De novo chimera detection, also referred to as reference-
264 free detection, represents an alternative computational paradigm that identifies
265 chimeric sequences without reliance on external reference databases. Instead of
266 comparing each query sequence to a curated collection of known, non-chimeric
267 sequences, de novo methods infer chimeras based on internal relationships among
268 the sequences present within the dataset itself. This approach is particularly
269 advantageous in studies of novel, under explored, or taxonomically diverse mi-
270 crobial communities where comprehensive reference databases are unavailable or
271 incomplete (Edgar, 2016; Edgar et al., 2011). The underlying assumption on this
272 method operates on the key biological principle that true biological sequences are
273 generally more abundant than chimeric artifacts. During PCR amplification, au-
274 thentic sequences are amplified early and tend to dominate the read pool, while

275 chimeric sequences form later resulting in the tendency to appear at lower relative
276 abundances compared to their true parental sequences. As such, the abundance
277 hierarchy is formed by treating the most abundant sequences as supposed parents
278 and testing whether less abundant sequences can be reconstructed as mosaics of
279 these dominant templates. In addition to abundance, de novo algorithms assess
280 compositional and structural similarity among sequences, examining whether cer-
281 tain regions of a candidate sequence align more closely with one high-abundance
282 sequence and other regions with a different one.

283 Both reference-based and de novo approaches are complementary rather than
284 mutually exclusive. Reference-based methods provide stability and reproducibility
285 when curated databases are available, whereas de novo methods offer flexibility
286 and independence for novel or highly diverse communities. In practice, many
287 modern bioinformatics pipelines combine both paradigms sequentially: an initial
288 de novo step identifies dataset-specific chimeras, followed by a reference-based pass
289 that removes remaining artifacts relative to established databases (Edgar, 2016).
290 These two methods of detection form the foundation of tools such as UCHIME
291 and later UCHIME2, exemplified by the dual capability of providing both modes
292 within a unified computational framework.

293 2.3.1 UCHIME

294 Developed by Edgar et al. (Edgar et al., 2011), UCHIME is one of the most widely
295 used computational tools for detecting chimeric sequences in amplicon sequencing
296 data. The UCHIME algorithm detects chimeras by evaluating how well a query
297 sequence (Q) can be explained as a mosaic of two parent sequences (A and B)

298 from a reference database. The query sequence is first divided into four non-
299 overlapping segments or chunks. Each chunk is independently searched against a
300 reference database that is assumed to be free of chimeras. The best matches to
301 each segment are collected, and from these results, two candidate parent sequences
302 are identified, typically the two sequences that best explain all chunks of the query.
303 Then a three-way alignment among the query (Q) and the two parent candidates
304 (A and B) is done. From this alignment, UCHIME attempts to find a chimeric
305 model (M) which is a hypothetical recombinant sequence formed by concatenating
306 fragments from A and B that best match the observed Q

307 Chimeric Alignment and Scoring

308 To decide whether a query is chimeric, UCHIME computes several alignment-
309 based metrics between Q, its top hit (T, the most similar known sequence), and
310 the chimeric model (M). The key differences are measured as: dQT or the number
311 of mismatches between the query and the top hit as well as dQM or the number
312 of mismatches between the query and the chimeric model. From these, a chimera
313 score is calculated to quantify how much better the chimeric model fits the query
314 compared to a single parent. If the model's similarity to Q exceeds a defined
315 threshold (typically $\geq 0.8\%$ better identity), the sequence is reported as chimeric.
316 A higher score indicates stronger evidence of chimerism, while lower scores suggest
317 that the sequence is more likely to be authentic.

318 In de novo mode, UCHIME applies an abundance-driven strategy. Only se-
319 quences at least twice as abundant as the query are considered as potential parents.
320 Non-chimeric sequences identified at each step are added iteratively to a growing

321 internal database for subsequent queries.

322 **Limitations of UCHIME**

323 Although UCHIME was a significant advancement in chimera detection, it has
324 notable limitations. According to (Edgar, 2016) and the UCHIME practical notes
325 (Edgar, n.d), many of the accuracy results reported in the original 2011 paper
326 were overly optimistic due to unrealistic benchmark designs that assumed com-
327 plete reference coverage and perfect sequence quality. In practice, UCHIME's
328 accuracy can decline when: (1) The reference database is incomplete or contains
329 erroneous entries. (2) Low-divergence chimeras are present, as these closely resem-
330 ble genuine biological variants. (3) Sequence datasets include residual sequencing
331 errors, leading to spurious alignments or misidentification; and (4) The abundance
332 ratio between parent and chimera is distorted by amplification bias. Additionally,
333 UCHIME tends to misclassify sequences as non-chimeric when parent sequences
334 are missing from the database. These limitations motivated the development of
335 UCHIME2.

336 **2.3.2 UCHIME2**

337 To overcome the limitations of its predecessor, UCHIME2 (Edgar, 2016) intro-
338 duced several methodological and algorithmic refinements that significantly en-
339 hanced the accuracy and reliability of chimera detection. One major improve-
340 ment lies in its approach to uncertainty handling. In earlier versions, sequences
341 with limited reference support were often incorrectly classified as non-chimeric,

342 increasing the likelihood of false negatives. UCHIME2 addresses this issue by
343 designating such ambiguous sequences as “unknown,” thereby providing a more
344 conservative and reliable classification framework.

345 Another notable advancement is the introduction of multiple application-
346 specific modes that allow users to tailor the algorithm’s performance to the
347 characteristics of their datasets. The following parameter presets: denoised,
348 balanced, sensitive, specific, and high-confidence, enable researchers to optimize
349 the balance between sensitivity and specificity according to the goals of their
350 analysis.

351 In comparative evaluations, UCHIME2 demonstrated superior detection per-
352 formance, achieving sensitivity levels between 93% and 99% and lower overall
353 error rates than earlier versions or other contemporary tools such as DECIPHER
354 and ChimeraSlayer. Despite these advances, the study also acknowledged a fun-
355 damental limitation in chimera detection: complete error-free identification is
356 theoretically unattainable. This is due to the presence of “perfect fake models,”
357 wherein genuine non-chimeric sequences can be perfectly reconstructed from other
358 reference fragments. This underscore the uncertainty in differentiating authentic
359 biological sequences from artificial recombinants based solely on sequence similar-
360 ity, emphasizing the need for continued methodological refinement and cautious
361 interpretation of results.

362 **2.3.3 CATch**

363 Early chimera detection programs such as UCHIME (Edgar et al., 2011) relied on
364 alignment-based and abundance-based heuristics to identify hybrid sequences in
365 amplicon data. However, researchers soon observed that different algorithms often
366 produced inconsistent predictions. A sequence might be identified as chimeric by
367 one tool but classified as non-chimeric by another, resulting in unreliable filtering
368 outcomes across studies.

369 To address these inconsistencies, (Mysara, Saeys, Leys, Raes, & Monsieurs,
370 2015) developed the Classifier for Amplicon Tool Chimeras (CATCh), which rep-
371 resents the first ensemble machine learning system designed for chimera detection
372 in 16S rRNA amplicon sequencing. Rather than depending on a single detec-
373 tion strategy, CATCh integrates the outputs of several established tools, includ-
374 ing UCHIME, ChimeraSlayer, DECIPHER, Pintail, and Perseus. The individual
375 scores and binary decisions generated by these tools are used as input features for
376 a supervised learning model. The algorithm employs a Support Vector Machine
377 (SVM) with a Pearson VII Universal Kernel (PUK) to determine optimal weight-
378 ings among the input features and to assign each sequence a probability of being
379 chimeric.

380 Benchmarking in both reference-based and de novo modes demonstrated signif-
381 icant performance improvements. CATCh achieved sensitivities of approximately
382 85 percent in reference-based mode and 92 percent in de novo mode, with corre-
383 sponding specificities of approximately 96 percent and 95 percent. These results
384 indicate that CATCh detected 7 to 12 percent more chimeras than any individual
385 algorithm while maintaining high precision. Integration of CATCh into amplicon-

386 processing pipelines also reduced operational taxonomic unit (OTU) inflation by
387 23 to 35 percent, producing diversity estimates that more closely reflected true
388 community composition.

389 2.3.4 ChimPipe

390 Among the available tools for chimera detection, ChimPipe is a bioinformatics
391 pipeline developed to identify chimeric sequences such as fusion genes and
392 transcription-induced chimeras from paired-end RNA sequencing data. It uses
393 both discordant paired-end reads and split-read alignments to improve the ac-
394 curacy and sensitivity of detecting fusion genes, trans-splicing events, and read-
395 through transcripts (Rodriguez-Martin et al., 2017). By combining these two
396 sources of information, ChimPipe achieves better precision than methods that
397 depend on a single type of signal.

398 The pipeline works with many eukaryotic species that have available genome
399 and annotation data, making it a versatile tool for studying chimera evolution
400 and transcriptome structure (Rodriguez-Martin et al., 2017). It can also predict
401 multiple isoforms for each gene pair and identify breakpoint coordinates that are
402 useful for reconstructing and verifying chimeric transcripts. Tests using both
403 simulated and real datasets have shown that ChimPipe maintains high accuracy
404 and reliable performance.

405 ChimPipe’s modular design lets users adjust parameters to fit different se-
406 quencing protocols or organism characteristics. Experimental results have con-
407 firmed that many chimeric transcripts detected by the tool correspond to func-

408 tional fusion proteins, showing its value for understanding chimera biology and
409 its potential applications in disease research (Rodriguez-Martin et al., 2017).

410 **2.4 Machine Learning Approaches for Chimera 411 and Sequence Quality Detection**

412 Traditional chimera detection tools rely primarily on heuristic or alignment-based
413 rules. Recent advances in machine learning (ML) have demonstrated that mod-
414 els trained on sequence-derived features can effectively capture compositional and
415 structural patterns in biological sequences. Although most existing ML systems
416 such as those used for antibiotic resistance prediction, taxonomic classification,
417 or viral identification are not specifically designed for chimera detection, they
418 highlight how data-driven models can outperform similarity-based heuristics by
419 learning intrinsic sequence signatures. In principle, ML frameworks can inte-
420 grate diverse indicators such as k-mer frequencies, GC-content variation, and
421 split-alignment metrics to identify subtle anomalies that may indicate a chimeric
422 origin (Arango et al., 2018; Liang, Bible, Liu, Zou, & Wei, 2020; Ren et al., 2020).

423 **2.4.1 Feature-Based Representations of Genomic Se- 424 quences**

425 In genomic analysis, feature extraction converts DNA sequences into numerical
426 representations suitable for ML algorithms. A common approach is k-mer fre-
427 quency analysis, where normalized k-mer counts form the feature vector (Vervier,

428 2015). These features effectively capture local compositional patterns that often
429 differ between authentic and chimeric reads. In particular, deviations in k-mer
430 profiles between adjacent read segments can serve as a compositional signature
431 of template-switching events. Additional descriptors such as GC content and
432 sequence entropy can further distinguish sequence types; in metagenomic classifi-
433 cation and virus detection, k-mer-based features have shown strong performance
434 and robustness to noise (Ren et al., 2020; Vervier, 2015). For chimera detection
435 specifically, abrupt shifts in GC or k-mer composition along a read can indicate
436 junctions between parental fragments. Windowed feature extraction enables mod-
437 els to capture these discontinuities that rule-based algorithms may overlook.

438 Machine learning models can also leverage alignment-derived features such as
439 the frequency of split alignments, variation in mapping quality, and local cover-
440 age irregularities. Split reads and discordant read pairs are classical signatures
441 of genomic junctions and have been formalized in probabilistic frameworks for
442 structural-variant discovery that integrate multiple evidence types (Layer, Hall, &
443 Quinlan, 2014). Similarly, long-read tools such as Sniffles employ split-alignment
444 and coverage anomalies to accurately localize breakpoints (Sedlazeck et al., 2018).
445 Modern aligners such as Minimap2 (Li, 2018) output supplementary (SA tags) and
446 secondary alignments as well as chaining and alignment-score statistics that can
447 be summarized into quantitative predictors for machine-learning models. These
448 alignment-signal features are particularly relevant to PCR-induced mitochondrial
449 chimeras, where template-switching events produce reads partially matching dis-
450 tinct regions of the same or related genomes. Integrating such cues within a
451 supervised-learning framework enables artifact detection even in datasets lacking
452 complete or perfectly assembled references.

453 A further biologically grounded descriptor is micro-homology length at puta-
454 tive junctions. Micro-homology refers to short, shared sequences (often in the
455 range of a few to tens of base pairs) that are near breakpoints and mediate
456 non-canonical repair or template-switch mechanisms. Studies of double strand
457 break repair and structural variation have demonstrated that the length of micro-
458 homology correlates with the likelihood of micro-homology-mediated end joining
459 (MMEJ) or fork-stalled template-switching pathways (Sfeir & Symington, 2015).
460 In the context of PCR-induced chimeras, template switching during amplifica-
461 tion often leaves short identical sequences at the junction of two concatenated
462 fragments. Quantifying the longest exact suffix–prefix overlap at each candidate
463 breakpoint thus provides a mechanistic signature of chimerism and complements
464 both compositional (k-mer) and alignment (SA count) features.

465 2.5 Synthesis of Chimera Detection Approaches

466 To provide an integrated overview of the literature discussed in this chapter, Ta-
467 ble 2.1 summarizes the major chimera detection studies, their methodological
468 approaches, and their known limitations. This consolidated comparison brings to-
469 gether reference-based approaches, de novo strategies, alignment-driven tools, en-
470 semble machine-learning systems, and general ML-based sequence-quality frame-
471 works. Presenting these methods side-by-side clarifies their performance bound-
472 aries and highlights the unresolved challenges that persist in mitochondrial genome
473 analysis and chimera detection.

Table 2.1: Summary of Existing Methods and Research

Gaps

Method/Study	Scope/Approach	Limitations
Reference-based Chimera Detection	Compares query sequences against curated, non-chimeric reference databases; identifies mosaic sequences by evaluating similarity to known templates.	Depends heavily on completeness and quality of reference databases; often fails when novel taxa or missing parent sequences are present; reduced accuracy for low-divergence chimeras.
De novo Chimera Detection	Identifies chimeras using only internal dataset relationships; relies on abundance patterns and compositional similarity; reconstructs sequences as mosaics of high-abundance parents.	Assumes true sequences are more abundant—fails when amplification bias distorts abundance; struggles with evenly abundant parental sequences; can misclassify highly similar true variants.

Method/Study	Scope/Approach	Limitations
UCHIME	Alignment-based chimera detection; segments query sequence, identifies parent candidates, performs 3-way alignment, and computes chimera scores; supports both reference-based and de novo modes.	Accuracy inflated in original benchmarks; suffers under incomplete databases; poor performance on low-divergence chimeras; sensitive to sequencing errors; misclassifies when parents are missing.
UCHIME2	Improved uncertainty handling; classifies ambiguous sequences as unknown; offers multiple sensitivity/specificity modes; more robust with incomplete references; higher sensitivity (93–99%).	Cannot achieve perfect accuracy due to “perfect fake models”; genuine variants may be indistinguishable from artificial recombinants; theoretical detection limit remains.
CATCh	First ML ensemble tool for 16S chimera detection; integrates outputs of UCHIME, ChimeraSlayer, DECIPHER, Pintail, Perseus via SVM classifier; significantly improves sensitivity and specificity.	Depends on performance of underlying tools; ML model limited to features they output; ensemble can still misclassify in datasets with extreme novelty or low coverage.

Method/Study	Scope/Approach	Limitations
ChimPipe	Pipeline for detecting fusion genes and transcript-derived chimeras in RNA-seq; uses discordant paired-end reads and split-alignments; predicts isoforms and breakpoint coordinates.	Designed for RNA-seq, not amplicons; needs high-quality genome and annotation; computationally heavier; limited to organisms with reference genomes.
Machine-Learning Sequence Quality & Chimera Detection (general)	Uses k-mer profiles, GC content shifts, entropy, split-read statistics, mapping quality variation, and micro-homology signatures as predictive features; identifies subtle artifacts missed by heuristics.	Requires labeled training data; model performance depends on feature engineering; may capture dataset-specific biases; limited generalization if training data is narrow or unrepresentative.

474 Across existing studies, no single approach reliably detects all forms of chimeric
 475 sequences, particularly those generated by PCR-induced template switching in
 476 mitochondrial genomes. Reference-based tools perform poorly when parental se-
 477 quences are absent; de novo methods rely strongly on abundance assumptions;
 478 alignment-based systems show reduced sensitivity to low-divergence chimeras; and
 479 ensemble methods inherit the limitations of their component algorithms. RNA-
 480 seq-oriented pipelines likewise do not generalize well to organelle data. Although
 481 machine learning approaches offer promising feature-based detection, they are
 482 rarely applied to mitochondrial genomes and are not trained specifically on PCR-

⁴⁸³ induced organelle chimeras. These limitations indicate a clear research gap: the
⁴⁸⁴ need for a specialized, feature-driven classifier tailored to mitochondrial PCR-
⁴⁸⁵ induced chimeras that integrates k-mer composition, split-alignment signals, and
⁴⁸⁶ micro-homology features to achieve more accurate detection than current heuristic
⁴⁸⁷ or alignment-based tools.

⁴⁸⁸ Chapter 3

⁴⁸⁹ Research Methodology

⁴⁹⁰ This chapter outlines and explains the specific steps and activities to be carried
⁴⁹¹ out in completing the project.

⁴⁹² 3.1 Research Activities

⁴⁹³ As illustrated in Figure 3.1, the researchers will carry out a sequence of compu-
⁴⁹⁴ tational procedures designed to detect PCR-induced chimeric reads in mitochon-
⁴⁹⁵ drial genomes. The process begins with the collection of mitochondrial reference
⁴⁹⁶ sequences from the NCBI database, which will serve as the foundation for gener-
⁴⁹⁷ ating simulated chimeric reads. These datasets will then undergo bioinformatics
⁴⁹⁸ pipeline development, which includes alignment, k-mer extraction, and homology-
⁴⁹⁹ based filtering to prepare the data for model construction. The machine-learning
⁵⁰⁰ model will subsequently be trained and tested using the processed datasets to
⁵⁰¹ assess its accuracy and reliability. Depending on the evaluation results, the model

502 will either be refined and retrained to improve performance or, if the metrics meet
503 the desired threshold, deployed for further validation and application.

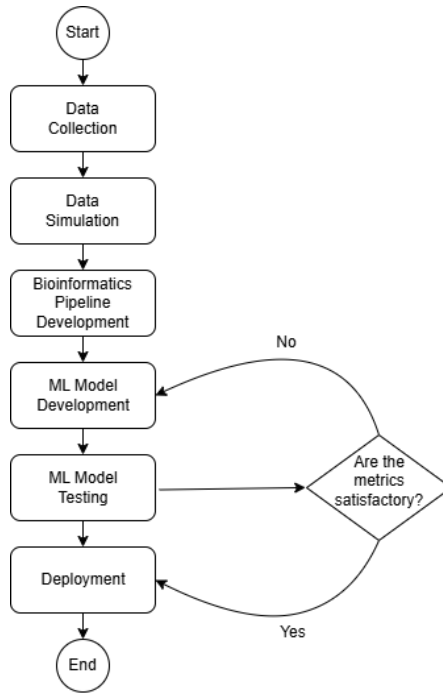


Figure 3.1: Process Diagram of Special Project

504 3.1.1 Data Collection

505 The researchers will collect mitochondrial genome reference sequences of *Sar-*
506 *dinella lemuru* from the National Center for Biotechnology Information (NCBI)
507 database. The downloaded files will be in FASTA format to ensure compatibility
508 with bioinformatics tools and subsequent analysis. The gathered sequences will
509 serve as the basis for generating simulated chimeric reads to be used in model
510 development.

511 The expected outcome of this process is a comprehensive dataset of *Sardinella*

512 *lemuru* mitochondrial reference sequences that will serve as the foundation for
513 the succeeding stages of the study. This step is scheduled to start in the first
514 week of November 2025 and is expected to be completed by the last week of
515 November 2025, with a total duration of approximately one (1) month.

516 3.1.2 Data Simulation

517 The researchers will simulate sequencing data using the reference sequences col-
518 lected from NCBI. Using `wgsim`, a total of 5,000 paired-end reads (R1 and R2)
519 will be generated from the reference genome and designated as clean reads. These
520 reads will be saved in FASTQ (`.fastq`) format. From the same reference, a Bash
521 script will be created to deliberately cut and reconnect portions of the sequence,
522 introducing artificial junctions that mimic chimeric regions. The manipulated
523 reference file, saved in FASTA (`.fasta`) format, will then be processed in `wgsim`
524 to simulate an additional 5,000 paired-end chimeric reads, also stored in FASTQ
525 (`.fastq`) format. The resulting read files will be aligned to the original reference
526 genome using SAMtools, generating SAM (`.sam`) or BAM (`.bam`) alignment files.
527 During this alignment process, clean reads will be labeled as “0,” while chimeric
528 reads will be labeled as “1” in a corresponding CSV (`.tsv`) file.

529 The expected outcome of this process is a complete set of clean and chimeric
530 paired-end reads prepared for subsequent analysis and model development. This
531 step is scheduled to start in the first week of November 2025 and is expected
532 to be completed by the last week of November 2025, with a total duration of
533 approximately one (1) month.

534 3.1.3 Bioinformatics Tools Pipeline

535 The researchers will obtain the necessary analytical features through the devel-
536 opment and implementation of a bioinformatics pipeline. This pipeline will serve
537 as a reproducible and modular workflow that accepts FASTQ and BAM inputs,
538 processes these through a series of analytical stages, and outputs tabular feature
539 matrices (TSV) for downstream machine learning. All scripts will be version-
540 controlled through GitHub, and computational environments will be standardized
541 using Conda to ensure cross-platform reproducibility. To promote transparency
542 and replicability, the exact software versions, parameters, and command-line ar-
543 guments used in each stage will be documented. To further ensure correctness
544 and adherence to best practices, the researchers will consult with bioinformatics
545 experts in Philippine Genome Center Visayas for validation of pipeline design,
546 feature extraction logic, and overall data integrity. This stage of the study is
547 scheduled to begin in the last week of November 2025 and conclude by the last
548 week of January 2026, with an estimated total duration of approximately two (2)
549 months.

550 The bioinformatics pipeline focuses on three principal features from the sim-
551 ulated and aligned sequencing data: (1) supplementary alignment count (SA
552 count), (2) k-mer composition difference between read segments, and (3) micro-
553 homology length at potential junctions. Each of these features captures a distinct
554 biological or computational signature associated with PCR-induced chimeras.

555 **Alignment and Supplementary Alignment Count**

556 This will be derived through sequence alignment using Minimap2, with subsequent
557 processing performed using SAMtools and `pysam` in Python. Sequencing reads
558 will be aligned to the *Sardinella lemuru* mitochondrial reference genome using
559 Minimap2 with the `-ax sr` preset (optimized for short reads). The output will
560 be converted and sorted using SAMtools, producing an indexed BAM file which
561 will be parsed using `pysam` to count the number of supplementary alignments
562 (SA tags) per read. Each read's mapping quality, number of split segments,
563 and alignment characteristics will be recorded in a corresponding TSV file. The
564 presence of multiple alignment loci within a single read, as reflected by a nonzero
565 SA count, serves as direct computational evidence of chimerism. Reads that
566 contain supplementary alignments or soft-clipped regions are strong candidates
567 for chimeric artifacts arising from PCR template switching or improper assembly
568 during sequencing.

569 **K-mer Composition Difference**

570 Chimeric reads often comprise fragments from distinct genomic regions, resulting
571 in a compositional discontinuity between segments. Comparing k-mer frequency
572 profiles between the left and right halves of a read allows detection of such abrupt
573 compositional shifts, independent of alignment information. This will be obtained
574 using Jellyfish, a fast k-mer counting software. For each read, the sequence will
575 be divided into two segments, either at the midpoint or at empirically determined
576 breakpoints inferred from supplementary alignment data, to generate left and right
577 sequence segments. Jellyfish will then compute k-mer frequency profiles (with $k =$

578 5 or 6) for each segment. The resulting k-mer frequency vectors will be normalized
579 and compared using distance metrics such as cosine similarity or Jensen–Shannon
580 divergence to quantify compositional disparity between the two halves of the same
581 read. The resulting difference scores will be stored in a structured TSV file.

582 **Micro-homology Length**

583 The micro-homology length will be computed using a custom Python script that
584 detects the longest exact suffix–prefix overlap within ± 30 base pairs surround-
585 ing a candidate breakpoint. This analysis identifies the number of consecutive
586 bases shared between the end of one segment and the beginning of another. The
587 presence and length of such micro-homology are classic molecular signatures of
588 PCR-induced template switching, where short identical regions (typically 3–15
589 base pairs) promote premature termination and recombination of DNA synthesis
590 on a different template strand. By quantifying micro-homology, the researchers
591 can assess whether the suspected breakpoint exhibits characteristics consistent
592 with PCR artifacts rather than true biological variants. Each read will therefore
593 be annotated with its corresponding micro-homology length, overlap sequence,
594 and GC content.

595 After extracting the three primary features, all resulting TSV files will be
596 joined using the read identifier as a common key to generate a unified feature ma-
597 trix. Additional read-level metadata such as read length, mean base quality, and
598 number of clipped bases will also be included to provide contextual information.
599 This consolidated dataset will serve as the input for subsequent machine-learning
600 model development and evaluation.

601 3.1.4 Machine-Learning Model Development

602 The classification component of MitoChime will employ two ensemble algo-
603 rithms—Random Forest (RF) and Extreme Gradient Boosting (XGBoost)—to
604 evaluate complementary learning paradigms. Random Forest applies bootstrap
605 aggregation (bagging) to reduce model variance and improve stability, whereas
606 XGBoost implements gradient boosting to minimize bias and capture complex
607 non-linear relationships among genomic features. Using both models enables a
608 balanced assessment of predictive performance and interpretability.

609 The dataset will be divided into training (80%) and testing (20%) subsets.
610 The training data will be used for model fitting and hyperparameter optimization
611 through five-fold cross-validation, in which the data are partitioned into five folds;
612 four folds are used for training and one for validation in each iteration. Perfor-
613 mance metrics will be averaged across folds, and the optimal parameters will be
614 selected based on mean cross-validation accuracy. The final models will then be
615 evaluated on the held-out test set to obtain unbiased performance estimates.

616 Model development and evaluation will be implemented in Python (ver-
617 sion 3.11) using the `scikit-learn` and `xgboost` libraries. Standard metrics
618 including accuracy, precision, recall, F1-score, and area under the ROC curve
619 (AUC) will be computed to quantify predictive performance. Feature-importance
620 analyses will be performed to identify the most discriminative variables contribut-
621 ing to chimera detection.

622 3.1.5 Validation and Testing

623 Validation will involve both internal and external evaluations. Internal validation
624 will be achieved through five-fold cross-validation on the training data to verify
625 model generalization and reduce variance due to random sampling. External
626 validation will be achieved through testing on the 20% hold-out dataset derived
627 from the simulated reads, which will serve as an unbiased benchmark to evaluate
628 how well the trained models generalize to unseen data. All feature extraction and
629 preprocessing steps will be performed using the same bioinformatics pipeline to
630 ensure consistency and comparability across validation stages.

631 Comparative evaluation between the Random Forest and XGBoost classifiers
632 will establish which model achieves superior predictive accuracy and computa-
633 tional efficiency under identical data conditions.

634 3.1.6 Documentation

635 Comprehensive documentation will be maintained throughout the study to en-
636 sure transparency, reproducibility, and scientific integrity. All stages of the re-
637 search—including data acquisition, preprocessing, feature extraction, model train-
638 ing, and validation—will be systematically recorded. For each analytical step, the
639 corresponding parameters, software versions, and command-line scripts will be
640 documented to enable exact replication of results.

641 Version control and collaborative management will be implemented through
642 GitHub, which will serve as the central repository for all project files, including
643 Python scripts, configuration settings, and Jupyter notebooks. The repository

644 structure will follow standard research data management practices, with clear
645 directories for datasets, processed outputs, and analysis scripts. Changes will be
646 tracked through commit histories to ensure traceability and accountability.

647 Computational environments will be standardized using Conda, with environ-
648 ment files specifying dependencies and package versions to maintain consistency
649 across systems. Experimental workflows and exploratory analyses will be con-
650 ducted in Jupyter Notebooks, which facilitate real-time visualization, annotation,
651 and incremental testing of results.

652 For the preparation of the final manuscript and supplementary materials,
653 Overleaf (LaTeX) will be utilized to produce publication-quality formatting, con-
654 sistent referencing, and reproducible document compilation. The documentation
655 process will also include a project timeline outlining major milestones such as
656 data collection, simulation, feature extraction, model evaluation, and reporting to
657 ensure systematic progress and adherence to the research schedule.

658 3.2 Calendar of Activities

659 Table 3.1 presents the project timeline in the form of a Gantt chart, where each
660 bullet point corresponds to approximately one week of planned activity.

Table 3.1: Timetable of Activities

Activities (2025)	Nov	Dec	Jan	Feb	Mar	Apr	May
Data Collection and Simulation	• • •						
Bioinformatics Tools Pipeline	• •	• • •	• • •				
Machine Learning Development			• •	• • •	• • •	• •	
Testing and Validation						• •	• • •
Documentation	• • •	• • •	• • •	• • •	• • •	• • •	• • •

661 References

- 662 Anderson, S., Bankier, A., Barrell, B., Bruijn, M., Coulson, A., Drouin, J., ...
663 Young, I. (1981, 04). Sequence and organization of the human mitochondrial
664 genome. *Nature*, 290, 457-465. doi: 10.1038/290457a0
- 665 Arango, G., Garner, E., Pruden, A., Heath, L., Vikesland, P., & Zhang, L. (2018,
666 02). Deeparg: A deep learning approach for predicting antibiotic resistance
667 genes from metagenomic data. *Microbiome*, 6. doi: 10.1186/s40168-018
668 -0401-z
- 669 Bentley, D. R., Balasubramanian, S., Swerdlow, H. P., Smith, G. P., Milton, J.,
670 Brown, C. G., ... Smith, A. J. (2008). Accurate whole human genome
671 sequencing using reversible terminator chemistry. *Nature*, 456(7218), 53–
672 59. doi: 10.1038/nature07517
- 673 Bi, C., Shen, F., Han, F., Qu, Y., Hou, J., Xu, K., ... Yin, T. (2024, 01).
674 Pmat: an efficient plant mitogenome assembly toolkit using low-coverage
675 hifi sequencing data. *Horticulture Research*, 11(3), uhae023. Retrieved
676 from <https://doi.org/10.1093/hr/uhae023> doi: 10.1093/hr/uhae023
- 677 Boore, J. L. (1999). Animal mitochondrial genomes. *Nucleic Acids Research*,
678 27(8), 1767–1780. doi: 10.1093/nar/27.8.1767
- 679 Cameron, S. L. (2014). Insect mitochondrial genomics: Implications for evolution

- 680 and phylogeny. *Annual Review of Entomology*, 59, 95–117. doi: 10.1146/
681 annurev-ento-011613-162007
- 682 Dierckxsens, N., Mardulyn, P., & Smits, G. (2017). Novoplasty: de novo assembly
683 of organelle genomes from whole genome data. *Nucleic Acids Research*,
684 45(4), e18. doi: 10.1093/nar/gkw955
- 685 Edgar, R. C. (2016). Uchime2: improved chimera prediction for amplicon se-
686 quencing. *bioRxiv*. Retrieved from <https://api.semanticscholar.org/>
687 CorpusID:88955007
- 688 Edgar, R. C. (n.d.). Uchime in practice. Retrieved from https://www.drive5.com/usearch/manual7/uchime_practical.html
- 689
- 690 Edgar, R. C., Haas, B. J., Clemente, J. C., Quince, C., & Knight, R. (2011).
691 Uchime improves sensitivity and speed of chimera detection. *Bioinformatics*,
692 27(16), 2194–2200. doi: 10.1093/bioinformatics/btr381
- 693 Frenkel-Morgenstern, M., Lacroix, V., Ezkurdia, I., Levin, Y., Gabashvili, A.,
694 Prilusky, J., ... Valencia, A. (2012, 05). Chimeras taking shape: Potential
695 functions of proteins encoded by chimeric rna transcripts. *Genome research*,
696 22, 1231-42. doi: 10.1101/gr.130062.111
- 697 Glenn, T. C. (2011). Field guide to next-generation dna sequencers. *Molecular
698 Ecology Resources*, 11(5), 759–769. doi: 10.1111/j.1755-0998.2011.03024.x
- 699 Gonzalez, J. M., Zimmermann, J., & Saiz-Jimenez, C. (2004, 09). Evalu-
700 ating putative chimeric sequences from pcr-amplified products. *Bioin-
701 formatics*, 21(3), 333-337. Retrieved from <https://doi.org/10.1093/bioinformatics/bti008> doi: 10.1093/bioinformatics/bti008
- 702
- 703 Gray, M. W. (2012). Mitochondrial evolution. *Cold Spring Harbor perspectives
704 in biology*, 4. Retrieved from <https://doi.org/10.1101/cshperspect.a011403> doi: 10.1101/cshperspect.a011403
- 705

- 706 Hahn, C., Bachmann, L., & Chevreux, B. (2013). Reconstructing mitochondrial
707 genomes directly from genomic next-generation sequencing reads—a baiting
708 and iterative mapping approach. *Nucleic Acids Research*, *41*(13), e129. doi:
709 10.1093/nar/gkt371
- 710 Jin, J.-J., Yu, W.-B., Yang, J., Song, Y., dePamphilis, C. W., Yi, T.-S., & Li,
711 D.-Z. (2020). Getorganelle: a fast and versatile toolkit for accurate de
712 novo assembly of organelle genomes. *Genome Biology*, *21*(1), 241. doi:
713 10.1186/s13059-020-02154-5
- 714 Judo, M. S. B., Wedel, W. R., & Wilson, B. H. (1998). Stimulation and sup-
715 pression of pcr-mediated recombination. *Nucleic Acids Research*, *26*(7),
716 1819–1825. doi: 10.1093/nar/26.7.1819
- 717 Labrador, K., Agmata, A., Palermo, J. D., Ravago-Gotanco, R., & Pante, M. J.
718 (2021). Mitochondrial dna reveals genetically structured haplogroups of
719 bali sardinella (sardinella lemuру) in philippine waters. *Regional Studies in*
720 *Marine Science*, *41*, 101588. doi: 10.1016/j.rsm.2020.101588
- 721 Layer, R., Hall, I., & Quinlan, A. (2014, 10). Lumpy: A probabilistic framework
722 for structural variant discovery. *Genome Biology*, *15*. doi: 10.1186/gb-2014
723 -15-6-r84
- 724 Li, H. (2018, 05). Minimap2: pairwise alignment for nucleotide sequences. *Bioin-*
725 *formatics*, *34*(18), 3094-3100. Retrieved from <https://doi.org/10.1093/bioinformatics/bty191>
726 doi: 10.1093/bioinformatics/bty191
- 727 Liang, Q., Bible, P. W., Liu, Y., Zou, B., & Wei, L. (2020, 02). Deepmi-
728 crobes: taxonomic classification for metagenomics with deep learning. *NAR*
729 *Genomics and Bioinformatics*, *2*(1), lqaa009. Retrieved from <https://doi.org/10.1093/nargab/lqaa009>
730 doi: 10.1093/nargab/lqaa009
- 731 Metzker, M. L. (2010). Sequencing technologies — the next generation. *Nature*

- 732 *Reviews Genetics*, 11(1), 31–46. doi: 10.1038/nrg2626
- 733 Mysara, M., Saeys, Y., Leys, N., Raes, J., & Monsieurs, P. (2015). Catch,
734 an ensemble classifier for chimera detection in 16s rrna sequencing stud-
735 ies. *Applied and Environmental Microbiology*, 81(5), 1573-1584. Retrieved
736 from <https://journals.asm.org/doi/abs/10.1128/aem.02896-14> doi:
737 10.1128/AEM.02896-14
- 738 Qin, Y., Wu, L., Zhang, Q., Wen, C., Nostrand, J. D. V., Ning, D., ... Zhou, J.
739 (2023). Effects of error, chimera, bias, and gc content on the accuracy of
740 amplicon sequencing. *mSystems*, 8(6), e01025-23. Retrieved from <https://journals.asm.org/doi/abs/10.1128/msystems.01025-23> doi: 10.1128/
741 msystems.01025-23
- 742 Qiu, X., Wu, L., Huang, H., McDonel, P. E., Palumbo, A. V., Tiedje, J. M., &
743 Zhou, J. (2001). Evaluation of pcr-generated chimeras, mutations, and het-
744 eroduplexes with 16s rrna gene-based cloning. *Applied and Environmental
745 Microbiology*, 67(2), 880–887. doi: 10.1128/AEM.67.2.880-887.2001
- 746 Ren, J., Song, K., Deng, C., Ahlgren, N., Fuhrman, J., Li, Y., ... Sun, F. (2020,
747 01). Identifying viruses from metagenomic data using deep learning. *Quan-
748 titative Biology*, 8. doi: 10.1007/s40484-019-0187-4
- 749 Rodriguez-Martin, B., Palumbo, E., Marco-Sola, S., Griebel, T., Ribeca, P.,
750 Alonso, G., ... Djebali, S. (2017, 01). Chimpipe: Accurate detection of
751 fusion genes and transcription-induced chimeras from rna-seq data. *BMC
752 Genomics*, 18. doi: 10.1186/s12864-016-3404-9
- 753 Rognes, T., Flouri, T., Nichols, B., Quince, C., & Mahé, F. (2016). Vsearch: a
754 versatile open source tool for metagenomics. *PeerJ*, 4, e2584. doi: 10.7717/
755 peerj.2584
- 756 Sedlazeck, F., Rescheneder, P., Smolka, M., Fang, H., Nattestad, M., von Haeseler,
757

- 758 A., & Schatz, M. (2018, 06). Accurate detection of complex structural
759 variations using single-molecule sequencing. *Nature Methods*, 15. doi: 10
760 .1038/s41592-018-0001-7
- 761 Sfeir, A., & Symington, L. S. (2015). Microhomology-mediated end joining: A
762 back-up survival mechanism or dedicated pathway? *Trends in Biochemical
763 Sciences*, 40(11), 701-714. Retrieved from <https://www.sciencedirect.com/science/article/pii/S0968000415001589> doi: <https://doi.org/10.1016/j.tibs.2015.08.006>
- 764 Vervier, M. P. T. M. V. J. B. . V. J. P., K. (2015). Large-scale machine learning
765 for metagenomics sequence classification. *Bioinformatics*, 32, 1023 - 1032.
766 Retrieved from <https://api.semanticscholar.org/CorpusID:9863600>
- 767 Willette, D., Bognot, E., Mutia, M. T., & Santos, M. (2011). *Biology and ecology
768 of sardines in the philippines: A review* (Vol. 13; Tech. Rep. No. 1). NFRDI
769 Technical Paper Series. Retrieved from <https://nfrdi.da.gov.ph/tpjf/etc/Willette%20et%20al.%20Sardines%20Review.pdf>
- 770
- 771
- 772